Editors' Suggestion | Featured in Physics

Experimental Verification of Dissipation-Time Uncertainty Relation

L.-L. Yan,[1] J.-W. Zhang,[2,3,4] M.-R. Yun,[1] J.-C. Li,[2,3] G.-Y. Ding,[2,3] J.-F. Wei,[1] J.-T. Bu,[2,3] B. Wang,[2,3] L. Chen,[2,4] S.-L. Su,[1,*] F. Zhou,[2,4,†] Y. Jia,[1,5] E.-J. Liang,[1] and M. Feng[2,1,3,4,‡]

[1]*School of Physics, Zhengzhou University, Zhengzhou 450001, China*

[2]*State Key Laboratory of Magnetic Resonance and Atomic and Molecular Physics, Wuhan Institute of Physics and Mathematics, Innovation Academy of Precision Measurement Science and Technology, Chinese Academy of Sciences, Wuhan 430071, China*

[3]*School of Physics, University of the Chinese Academy of Sciences, Beijing 100049, China*

[4]*Research Center for Quantum Precision Measurement, Guangzhou Institute of Industry Technology, Guangzhou 511458, China*

[5]*Key Laboratory for Special Functional Materials of Ministry of Education, and School of Materials and Engineering, Henan University, Kaifeng 475001, China*

(Received 25 August 2021; revised 8 November 2021; accepted 14 January 2022; published 4 February 2022)

Dissipation is vital to any cyclic process in realistic systems. Recent research focus on nonequilibrium processes in stochastic systems has revealed a fundamental trade-off, called dissipation-time uncertainty relation, that entropy production rate associated with dissipation bounds the evolution pace of physical processes [Phys. Rev. Lett. **125**, 120604 (2020)]. Following the dissipative two-level model exemplified in the same Letter, we experimentally verify this fundamental trade-off in a single trapped ultracold $^{40}Ca^{+}$ ion using elaborately designed dissipative channels, along with a postprocessing method developed in the data analysis, to build the effective nonequilibrium stochastic evolutions for the energy transfer between two heat baths mediated by a qubit. Since the dissipation-time uncertainty relation imposes a constraint on the quantum speed regarding entropy flux, our observation provides the first experimental evidence confirming such a speed restriction from thermodynamics on quantum operations due to dissipation, which helps us further understand the role of thermodynamical characteristics played in quantum information processing.

DOI: 10.1103/PhysRevLett.128.050603

Since any realistic system is subject to the coupling to an uncontrollable environment, the irreversibility of state evolution is overwhelming in quantum operations [1–3]. In this context, dissipation is essential to any physical process, which initializes the system, sometimes helps for accelerating state evolution, and also affects measurement precision. On the other hand, to keep quantum properties, people are required to work fast in quantum systems for suppressing detrimental influence from dissipation and/or decoherence, indicating that nonequilibrium dynamics dominates quantum processes [4]. However, how fast the quantum operations can be performed is not fully determined by quantum technical efforts, but is also constrained by something beyond quantumness [5–7]. In fact, the nonequilibrium processes in thermodynamics have drawn much attention over the past decades [8–12]. In particular, due to rapid progress in quantum technology, understanding the nonequilibrium thermodynamic process at the quantum level has recently become a hot topic [13–18]. Extended to the quantum regime, most thermodynamic quantities should be retraced, and thus most restrictions of the original thermodynamics have to be reformulated [19–27].

The present Letter concentrates on nonequilibrium thermodynamic processes in the quantum regime, which are strongly constrained by dissipation. We have already noticed some thermodynamic uncertainty relations proposed recently [28–41], indicating that precision in nonequilibrium dynamics is intrinsically constrained by dissipation or measurements. Actually, the similar thermodynamic limitation also exits for quantum speed, as discovered very recently [42], by a dissipation-time uncertainty relation, imposing an upper bound on quantum speed regarding any stochastic dynamics.

Here we report our verification of this dissipation-time uncertainty relation at atomic level via experimental manipulation of a trapped-ion system, which basically follows the dissipative two-level model exemplified in [42]. Although the uncertainty relation applies to both classical and quantum systems, our verification using a single-ion quantum system is based on following considerations. First, quantum processes are more fundamental than classical counterparts in physical transformations and evolutions. Second, the trapped-ion system can be controlled in high precision, which provides an ideal platform to explore quantum dynamics with ultimate accuracy. As a result, besides a creditable test of this fundamental trade-off, our experimental execution would also be helpful for further understanding thermodynamic characteristics in the quantum regime.

To demonstrate the required stochastic trajectories of thermodynamic processes, we first construct an effective energy transfer between two heat baths mediated through a qubit by elaborately designing four dissipative channels in

the ultracold trapped ion. Then we develop a discretization-repetition ensemble average method for postprocessing data, which could effectively deal with some intractable difficulties in our experimental implementation, such as the successive detection of single photon dissipation and the unexpected population leakage in the dissipative channels. As such, our execution, actually based on an effective two-level model involving controllable drive and dissipation as elucidated below, could be perfectly precise, which ensures a reliable evidence in our test of the new trade-off at the most fundamental level.

Before specifying our experimental scheme and system, we first elucidate briefly the theory of the dissipation-time uncertainty relation proposed in [42]. Consider a process that describes an observable O to first pass a given threshold D within a specific duration t [43–45]. Because of the fluctuation in the nonequilibrium dynamic process, stochastic trajectories of the process may pass the threshold or not within the duration. Here we define the survival probability of the process by $p^s(t) \coloneqq P(\tau > t)$, representing the probability of the trajectory's first passage time τ longer than t [46]. By this definition, the instantaneous rate of the process is defined as $r(t) \coloneqq -\dot{p}^s(t)/p^s(t)$ and the corresponding time-averaged rate is $\bar{r}(t) \coloneqq (1/t)\int_0^t r(t')dt'$ [47]. Provided that the time reversed process is exponentially rare, implying negligible entropy production rate in the reverse process, the entropy flux of the stationary dynamics primarily comes from the entropy flux $\dot{S}_e$ in the heat baths [48,49]. As such, the entropy flux sets an upper bound on the time-averaged rate, i.e.,

$$\dot{S}_e/k_B \geq \bar{r}(t), \tag{1}$$

where k_B is the Boltzmann constant. When the mean time to accomplish the process is finite, i.e., $\mathcal{T} \coloneqq \int_0^\infty p^s(t)dt < \infty$ [46], the entropy flux and mean time of the process obey the following dissipation-time uncertainty relation [42]:

$$\dot{S}_e\mathcal{T} \geq k_B, \tag{2}$$

which imposes a thermodynamic restriction for nonequilibrium processes; i.e., for a nonequilibrium process within a given time $\mathcal{T}$, the system has to dissipate at least $k_B/\mathcal{T}$ entropy flux to the reservoir [50].

To test this newly discovered fundamental trade-off in Eq. (2), we consider a quantum model involving a two-level system coupled to two heat baths with the energy transfer from the hot bath to the cold bath mediated by the two-level system. The transfer rates associated with different baths and states are given by $\omega^\nu_{i\to j} = e^{-\beta_\nu(\epsilon_j-\epsilon_i)/2}$ ($i, j = e, g$, and $\nu = h, c$) with the energy difference $\epsilon = \epsilon_e - \epsilon_g$ and $\beta_c > \beta_h$. In this context, the energy flow from the hot bath to the cold bath within a fixed time δ can be expressed as [51]

$$O = \epsilon\int_0^\delta dt'\left[\frac{dN^c_{e\to g}}{dt'} - \frac{dN^c_{g\to e}}{dt'}\right], \qquad D \in [E, +\infty), \tag{3}$$

where the Poisson process $dN^\nu_{i\to j}$ represents the Markovian jumps between these two states with the rate $w^\nu_{i\to j}$, E is an activation energy [52], and δ is the timescale over which the activation energy is dissipated [42]. Then, the entropy flow can be analytically solved as $\dot{S}_e = k_B\epsilon(\beta_h - \beta_c)(e^{\beta_h\epsilon/2} - e^{\beta_c\epsilon/2})/[1 + e^{(\beta_h+\beta_c)\epsilon/2}]$ [42,51].

Our experiment is carried out in the single $^{40}Ca^+$ ion confined in a linear Paul trap with axial frequency $\omega_z/2\pi = 1.1$ MHz and radial frequency $\omega_r/2\pi = 1.6$ MHz [19]. By applying a magnetic field of approximately 3.4 G along the axial direction, we define a quantization axis with the final average phonon number $\bar{n} < 1$ after sideband cooling. The two-level system is encoded in the two sublevels of the ground state, i.e., $|4^2S_{1/2}, m_J = -1/2\rangle$ (labeled as $|g\rangle$) and $|4^2S_{1/2}, m_J = +1/2\rangle$ (labeled as $|e\rangle$) with m_J denoting the magnetic quantum number. Because of lack of the necessary decay paths required to construct the energy transfer processes induced by the two heat baths, we introduce two extra energy levels, i.e., the sublevels of the metastable state $|3^2D_{5/2}\rangle$ and the excited state $|4^2P_{3/2}\rangle$, as sketched in Fig. 1, to produce the effective dissipative channels, where the details can be found in the Supplemental Material [51]. To create valid dissipative channels, the coherent processes need to be suppressed. In this case, we have analytically solved the effective decay rates in the four-level system [51],

$$\gamma^c_i = \frac{\Omega^2_{i1}\Gamma_i}{\Omega^2_{i2}}, \qquad \gamma^h_k = \frac{\Omega^2_{k1}\Gamma_{k1}}{\sqrt{\Omega^4_{k2} + 5\Omega^2_{k1}\Gamma^2_{k2}}}, \tag{4}$$

with subscripts $i = 1, 2$ and $k = 3, 4$, and the superscript c (h) denoting the cold (hot) heat bath. Here $\gamma^c_{1,2}$ ($\gamma^h_{3,4}$) represents $\gamma^c_{e\to g, g\to e}$ ($\gamma^h_{e\to g, g\to e}$) in Fig. 1.

The experimental results for these dissipative channels are presented in Fig. 2, where the effective decay rates in different dissipative channels fully cover the necessary condition $\gamma^c_{e\to g} > \gamma^h_{e\to g} > \gamma^h_{g\to e} > \gamma^c_{g\to e}$. Meanwhile, the experimental results also well satisfy the analytical solution of the effective decay rates as predicted by Eq. (4). To connect the transfer rates with the decay rates of the four dissipative channels, we assume $\gamma^c_{e\to g} = \mathcal{R}_c\omega^c_{e\to g}$, $\gamma^c_{g\to e} = \mathcal{R}_c\omega^c_{g\to e}$, $\gamma^h_{e\to g} = \mathcal{R}_h\omega^h_{e\to g}$, and $\gamma^h_{g\to e} = \mathcal{R}_h\omega^h_{g\to e}$, where $\mathcal{R}_{c,h} \coloneqq \sqrt{\gamma^{c,h}_{e\to g}\gamma^{c,h}_{g\to e}}$ represents the proportionality coefficients for cold and hot heat baths. In the equilibrium system balanced by the cold and hot heat baths, $\mathcal{R}_c = \mathcal{R}_h$ should be satisfied. The decay rates observed in Fig. 2, however, do not strictly meet the proportionality condition, which have the deviation of $\mathcal{D} = |\gamma^c_{e\to g}\gamma^c_{g\to e} - \gamma^h_{e\to g}\gamma^h_{g\to e}|$. Based on the condition $\mathcal{D} < 1$, we choose the appropriate

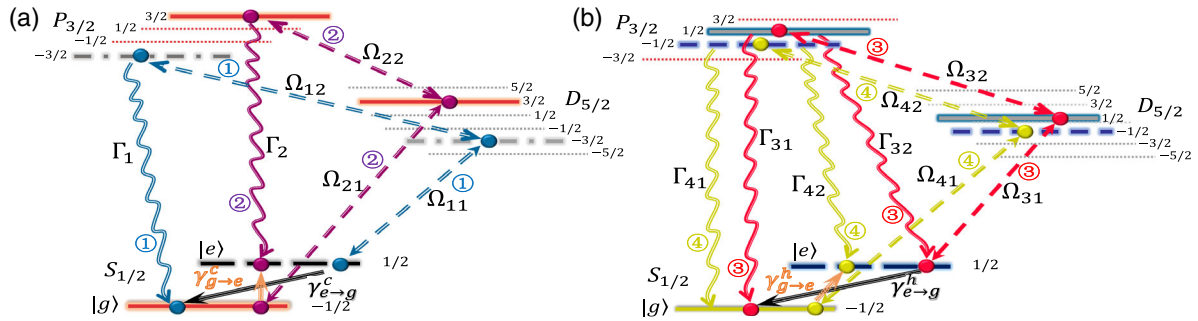

FIG. 1. Level schemes constructed for an effective two-level system in contact with two heat baths in the trapped $^{40}Ca^+$ ion. (a) Levels constructed for the dissipative channels regarding cold heat bath. (b) Levels constructed for the dissipative channels regarding hot heat bath. Each dissipative channel is constructed by two heterochromatic lasers with the wavelengths of 729 and 854 nm, respectively, where the Rabi frequency Ω_{n1} (Ω_{n2}), with $n = 1$, 2, 3, and 4, represents the resonant coupling of a sublevel of the ground state (metastable state) to a sublevel of the metastable state (excited state), and the decay of the excited state to the ground state accomplishes the effective procedure of the dissipative channel. Here, we set $\Omega_{n2} \gg \Omega_{n1}$ to guarantee the steady dissipative process, and the lifetime of the excited state is 6.9 ns; i.e., the decay rate $\Gamma/2\pi = 23.1$ MHz, while the metastable state has a negligible decay rate due to 1.2 s lifetime.

parameter groups of $\gamma^{c,h}_{e\to g}$ and $\gamma^{c,h}_{g\to e}$, and obtain 20 parameter groups using the accessible decay rates in Fig. 2. For our purpose, we exemplify the four groups listed in Table I to verify the dissipation-time uncertainty relation, as elucidated later.

To verify Eq. (2), however, we have to construct and then observe the required stochastic trajectories experimentally, which is challenging in our system. First, the four dissipative channels are constructed by the same four levels, which makes it unavailable that all the channels are independent and work simultaneously as required by Eq. (2). Second, there are population leakages in each of the designed dissipative channels [51], yielding the system to be unavailable for long-time evolution. Third, continuous observation of single-photon dissipation regarding each of the four channels, which is different from the electronic shelving-amplification measurement, is unavailable by the fluorescence collection in the ion-trap system.

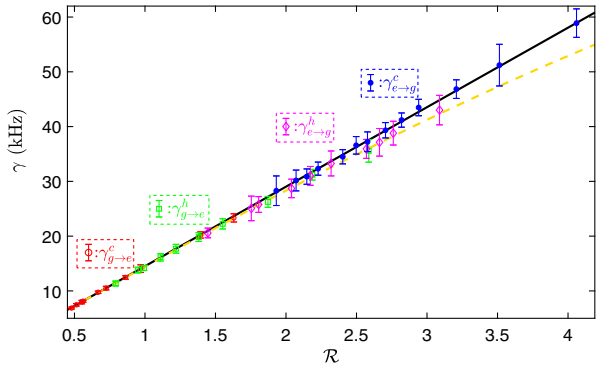

FIG. 2. Decay rates in different dissipative channels constructed in the trapped $^{40}Ca^+$ ion, where the black solid (orange dashed) line indicates the analytical solutions of the channels with the single(double)-decay processes in Eq. (4), and the experimental data are represented by blue dots, red circles, magenta diamonds, and green squares corresponding to the dissipative channels ①, ②, ③, and ④, respectively. Here the experimental data are measured with 4000 repetitions and the parameter in the horizontal axis is defined as $\mathcal{R}/10^4 = \Omega^2_{k1}/\Omega^2_{k2}$ with k denoting the kth channel.

To deal with these problems, we have developed a postprocessing method, based on the quantum jump theory [53], to produce stochastic evolution trajectories in data analysis, which can be called the discretization-repetition ensemble average method. We split the whole duration of evolution into n pieces, where no serious leakage occurs within the time period τ of each piece. By this way, we may employ Eq. (3) to quantify the energy transfer in each of these time durations, and then connect the durations, depending on certain random numbers, to construct a stochastic evolution trajectory over the time period $n\tau$. Under the assumption that the stochastic processes are independent of each other, we can acquire an equilibrium process by averaging all the possible evolutions.

For our purpose, we first have to compensate the loss due to population leakage (ε) and imperfect initial state preparation (ξ), which yields the modified probability $\tilde{P}_t = (P_t - \varepsilon)/(1 - \xi - \varepsilon)$, where P_t is acquired from the experimentally observed dataset of $\{0, 1\}$, and ε and ξ are given based on experimental observation, see details in the Supplemental Material [51]. With the renewed probability $\tilde{P}_t$, we may update the original experimental dataset by randomly substituting $(\tilde{P}_\tau - P_\tau)\mathcal{N}$ zero by one, where $\mathcal{N}$

TABLE I. Four typical decay groups for the accessible decay rates in units of kilohertz regarding the dissipative channels constructed in Fig. 1, with $1/\beta_{c,h}$ in units of $\epsilon = 9.5$ MHz.

Group	$\gamma^c_{e\to g}$	$\gamma^c_{g\to e}$	$\gamma^h_{e\to g}$	$\gamma^h_{g\to e}$	β_c	β_h
I	32.3(12)	23.3(7)	28.7(17)	26.2(9)	0.33(5)	0.09(7)
II	46.8(17)	9.7(3)	25.7(9)	17.7(8)	1.57(5)	0.37(6)
III	51.2(38)	6.9(2)	31(17)	11.4(4)	2.00(8)	1.00(6)
IV	41.2(13)	14.1(7)	35.9(17)	16.2(7)	1.07(6)	0.79(6)

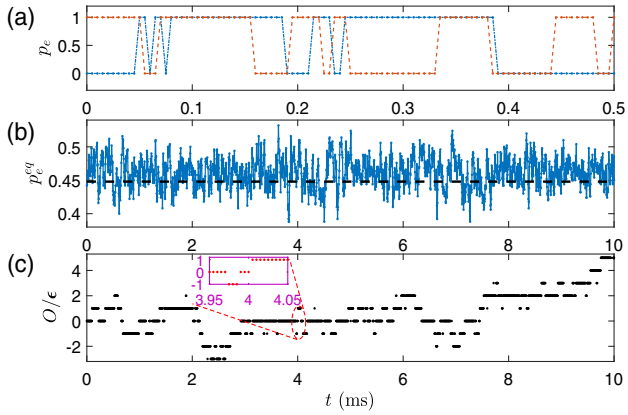

FIG. 3. (a) Two exemplified stochastic trajectories of the dissipative processes, started from $|g\rangle$ (blue line) or $|e\rangle$ (red line), obtained by the discretization-repetition ensemble average method. (b) Population in state $|e\rangle$ in the equilibrium process obtained by the ensemble average of 500 stochastic trajectories, where the dashed line indicates the analytical solution. (c) Energy flow in a single stochastic trajectory of the process, where a duration of 4 ms is amplified for scrutinizing the details. The experimental parameters are selected from group I of Table I. The ensemble case of the energy flow with evident characteristic that the time reversed process is rare can be found in Fig. S12 in the Supplemental Material [51].

represents the total number of the data in this set. Then for each time piece, we consider $\tau = 5\ \mu$s in terms of our experimental condition. For a certain trajectory, for instance, if the initial state of the first time piece is prepared in $|e\rangle$, the evolution along channel ① or ③ depends on a stochastic number in the interval [0, 1]. If the stochastic number is larger than 0.5, we choose the evolution along channel ①, where the experimental data are randomly chosen from the dataset of channel ① at the moment of 5 μs. Otherwise, the state evolves along channel ③. The second time piece gets started from the final state of the first counterpart with the evolution depending on another random number. The evolutions run similarly in succession for the rest of the pieces, as exemplified in Fig. 3(a). Finally, in terms of the population probability in the equilibrium state, we randomize $|g\rangle$ or $|e\rangle$ as the starting point of a trajectory. Averaging on large numbers of such trajectories, the equilibrium process can be obtained, see Fig. 3(b). Based on the treatments above, we have built the required stochastic evolution trajectories, where the employed random numbers regarding the trajectories represent the record of the single photon dissipation [see the inset of Fig. 4(a)]. As such, we directly obtain the energy flow as presented in Fig. 3(c).

Figure 4(a) demonstrates the survival probabilities of the processes with approximately exponential decays with respect to the evolution time, indicating negligible reverse processes. The influence from larger activation energy is reflected in the less steep survival probability curve, implying that more reverse processes are involved (particularly in the initial duration) and thus the energy transfer takes a longer time. Moreover, the time-averaged rate of the process presented in Fig. 4(b) is bounded by the entropy flux of the heat baths regarding the stationary dynamics, i.e., the bound in Eq. (1). In Fig. 4(b), we may see the violation of the bound at the initial part of the process, regarding the nonstationary dynamics, which does not invalidate Eq. (1) (more results can be found in the Supplemental Material [51]). Actually, considering the process with infinite time duration, we have witnessed in Fig. 5, with the four data groups acquired from Table I, that the entropy flux and the mean time of the process obey the dissipation-time uncertainty relation as quantified

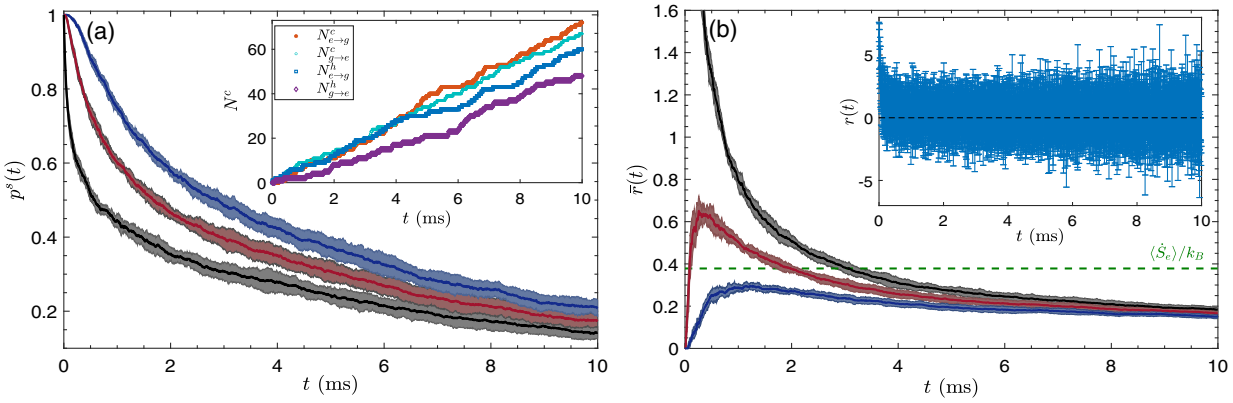

FIG. 4. (a) Time evolution of the survival probabilities $p^s(t)$ of the process trajectories associated with different activation energies. Inset: the energy transfer in a stochastic trajectory for four different types of Markovian jumps induced by the cold and hot heat baths. (b) Time-averaged rate $\bar{r}(t)$ of the energy transfer process for different activation energies, where the green dashed line denotes the entropy flux of the stationary dynamics. Inset: the instantaneous rate $r(t)$ for an activation energy $E = \epsilon$, obtained by the survival probability, shows the stochastic entropy flux, and the small imbalance between the positive and negative directions at the initial period also illustrates the nonequilibrium property of the process with the predominant positive process. (a),(b) The black, red, and blue curves correspond to $E = \epsilon, 2\epsilon$, and 3ϵ, respectively, where the shaded area indicates the uncertainty of the date due to errors. Here, we choose the experimental values of the dissipative channels from group I of Table I.

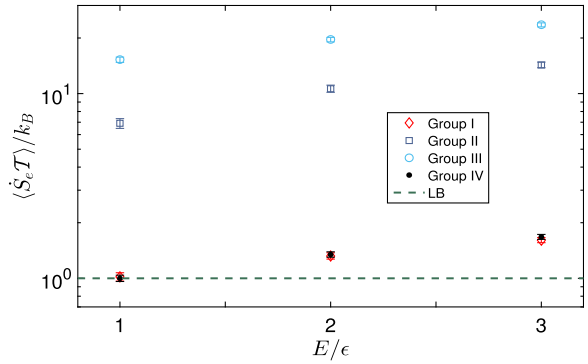

FIG. 5. Dissipation-time uncertainty relation under activation energy E, where the green dashed line indicates the lower bound (LB), i.e., k_B. The error bars represent statistical standard deviation of our experimental observation by 4000 measurements for each data point.

by Eq. (2). In particular, the data overlapping of groups I and IV indicates the tiny difference between their parameters $\beta_{c,h}$, which leads to saturating the lower bound due to very little entropy flow and time-average rate in these nearly equilibrium processes.

In summary, our experiment has provided the first single-atom evidence confirming the lower bound of entropy flux and process duration in the dissipative processes of stochastic systems. The developed postprocessing method in the data analysis would be useful in ion-trap systems for experimentally simulating more complicated nonequilibrium processes. We believe that our experimental verification at the atomic level will definitely be helpful for further understanding thermodynamic characteristics in the quantum regime, particularly when faster operations are expected in quantum information processing.

We thank Gianmaria Falasco and Massimiliano Esposito for enlightening discussion. This work was supported by Special Project for Research and Development in Key areas of Guangdong Province under Grant No. 2020B0303300001, by National Key Research and Development Program of China under Grant No. 2017YFA0304503, by National Natural Science Foundation of China under Grants No. U21A20434, No. 12074346, No. 12074390, No. 11835011, No. 11804375, No. 11804308, No. 11874328, No. 91421111, No. 11734018, No. 11774078, and No. 12074099, by Natural Science Foundation of Henan Province under Grants No. 202300410481 and No. 212300410085, and by K. C. Wong Education Foundation (GJTD-2019-15).

L.-L. Y. and J.-W. Z contributed equally to this work.

*slsu@zzu.edu.cn
†zhoufei@wipm.ac.cn
‡mangfeng@wipm.ac.cn

[1] N. Shiraishi and K. Saito, Information-Theoretical Bound of the Irreversibility in Thermal Relaxation Processes, Phys. Rev. Lett. **123**, 110603 (2019).
[2] J. W. Zhang, K. Rehan, M. Li, J. C. Li, L. Chen, S.-L. Su, L.-L. Yan, F. Zhou, and M. Feng, Single-atom verification of the information-theoretical bound of irreversibility at the quantum level, Phys. Rev. Research **2**, 033082 (2020).
[3] T. V. Vu and Y. Hasegawa, Geometrical Bounds of the Irreversibility in Markovian Systems, Phys. Rev. Lett. **126**, 010601 (2021).
[4] J. M. R. Parrondo, J. M. Horowitz, and T. Sagawa, Thermodynamics of information, Nat. Phys. **11**, 131 (2015).
[5] S. Deffner and S. Campbell, Quantum speed limits: From Heisenberg's uncertainty principle to optimal quantum control, J. Phys. A **50**, 453001 (2017).
[6] B. Shanahan, A. Chenu, N. Margolus, and A. Del Campo, Quantum Speed Limits across the Quantum-to-Classical Transition, Phys. Rev. Lett. **120**, 070401 (2018).
[7] M. Okuyama and M. Ohzeki, Quantum Speed Limit is Not Quantum, Phys. Rev. Lett. **120**, 070402 (2018).
[8] C. Jarzynski, Nonequilibrium Equality for Free Energy Differences, Phys. Rev. Lett. **78**, 2690 (1997).
[9] C. Jarzynski, Equilibrium free-energy differences from nonequilibrium measurements: A master-equation approach, Phys. Rev. E **56**, 5018 (1997).
[10] J. Liphardt, S. Dumont, S. B. Smith, I. T. Jr., and C. Bustamante, Equilibrium information from nonequilibrium measurements in an experimental test of Jarzynski's equality, Science **296**, 1832 (2002).
[11] G. E. Crooks, Entropy production fluctuation theorem and the nonequilibrium work relation for free energy differences, Phys. Rev. E **60**, 2721 (1999).
[12] D. Collin1, F. Ritort2, C. Jarzynski, S. B. Smith, I. Tinoco Jr, and C. Bustamante, Verification of the Crooks fluctuation theorem and recovery of RNA folding free energies, Nature (London) **437**, 231 (2005).
[13] J. Gemmer, M. Michel, and G. Mahler, *Quantum Thermodynamics* (Springer, Berlin, 2004).
[14] K. Maruyama, F. Nori, and V. Vedral, The physics of Maxwells demon and information, Rev. Mod. Phys. **81**, 1 (2009).
[15] M. Campisi, P. Hänggi, and P. Talkner, Quantum fluctuation relations: Foundations and applications, Rev. Mod. Phys. **83**, 771 (2011).
[16] D. von Lindenfels, O. Gräb, C. T. Schmiegelow, V. Kaushal, J. Schulz, Mark T. Mitchison, John Goold, F. Schmidt-Kaler, and U. G. Poschinger, Spin Heat Engine Coupled to a Harmonic-Oscillator Flywheel, Phys. Rev. Lett. **123**, 080602 (2019).
[17] John P. S. Peterson, Tiago B. Batalhäo, Marcela Herrera, Alexandre M. Souza, Roberto S. Sarthour, Ivan S. Oliveira, and Roberto M. Serra, Experimental Characterization of a Spin Quantum Heat Engine, Phys. Rev. Lett. **123**, 240601 (2019).
[18] M. Naghiloo, D. Tan, P. M. Harrington, J. J. Alonso, E. Lutz, A. Romito, and K. W. Murch, Heat and Work along Individual Trajectories of a Quantum Bit, Phys. Rev. Lett. **124**, 110604 (2020).
[19] L. L. Yan, T. P. Xiong, K. Rehan, F. Zhou, D. F. Liang, L. Chen, J. Q. Zhang, W. L. Yang, Z. H. Ma, and M. Feng,

Single-Atom Demonstration of the Quantum Landauer Principle, Phys. Rev. Lett. **120**, 210601 (2018).
[20] T. P. Xiong, L. L. Yan, F. Zhou, K. Rehan, D. F. Liang, L. Chen, W. L. Yang, Z. H. Ma, M. Feng, and V. Vedral, Experimental Verification of a Jarzynski-Related Information-Theoretic Equality Using a Single Trapped Ion, Phys. Rev. Lett. **120**, 010601 (2018).
[21] P. Faist, M. Berta, and F. Brandão, Thermodynamic Capacity of Quantum Processes, Phys. Rev. Lett. **122**, 200601 (2019).
[22] R. Sánchez, J. Splettstoesser, and Robert S. Whitney, Nonequilibrium System as a Demon, Phys. Rev. Lett. **123**, 216801 (2019).
[23] K. Beyer, K. Luoma, and W. T. Strunz, Steering Heat Engines: A Truly Quantum Maxwell Demon, Phys. Rev. Lett. **123**, 250606 (2019).
[24] K. Micadei, G. T. Landi, and E. Lutz, Quantum Fluctuation Theorems beyond Two-Point Measurements, Phys. Rev. Lett. **124**, 090602 (2020).
[25] D. Gupta, C. A. Plata, and A. Pal, Work Fluctuations and Jarzynski Equality in Stochastic Resetting, Phys. Rev. Lett. **124**, 110608 (2020).
[26] A. M. Timpanaro, J. P. Santos, and G. T. Landi, Landauer's Principle at Zero Temperature, Phys. Rev. Lett. **124**, 240601 (2020).
[27] P. Faist, M. Berta, and F. Brandão, Geometry of Work Fluctuations versus Efficiency in Microscopic Thermal Machines, Phys. Rev. Lett. **125**, 260601 (2020).
[28] A. C. Barato and U. Seifert, Thermodynamic Uncertainty Relation for Biomolecular Processes, Phys. Rev. Lett. **114**, 158101 (2015).
[29] J. M. Horowitz and T. R. Gingrich, Proof of the finite-time thermodynamic uncertainty relation for steady-state currents, Phys. Rev. E **96**, 020103(R) (2017).
[30] K. Proesmans and C. Van den Broeck, Discrete-time thermodynamic uncertainty relation, Europhys. Lett. **119**, 20001 (2017).
[31] A. Dechant and S. I. Sasa, Entropic bounds on currents in Langevin systems, Phys. Rev. E **97**, 062101 (2018).
[32] Y. Hasegawa and T. V. Vui, Fluctuation Theorem Uncertainty Relation, Phys. Rev. Lett. **123**, 110602 (2019).
[33] A. Timpanaro, G. Guarnieri, J. Goold, and G. T. Landi, Thermodynamic Uncertainty Relations from Exchange Fluctuation Theorems, Phys. Rev. Lett. **123**, 090604 (2019).
[34] G. Falasco, M. Esposito, and J.-C. Delvenne, Unifying thermodynamic uncertainty relations, New J. Phys. **22**, 053046 (2020).
[35] K. Liu, Z. Gong, and M. Ueda, Thermodynamic Uncertainty Relation for Arbitrary Initial States, Phys. Rev. Lett. **125**, 140602 (2020).
[36] Y. Hasegawa, Quantum Thermodynamic Uncertainty Relation for Continuous Measurement, Phys. Rev. Lett. **125**, 050601 (2020).
[37] T. V. Vu and Y. Hasegawa, Thermodynamic uncertainty relations under arbitrary control protocols, Phys. Rev. Research **2**, 013060 (2020).
[38] T. Koyuk and U. Seife, Thermodynamic Uncertainty Relation for Time-Dependent Driving, Phys. Rev. Lett. **125**, 260604 (2020).
[39] J. M. Horowitz and T. R. Gingrich, Thermodynamic uncertainty relations constrain non-equilibrium fluctuations, Nat. Phys. **16**, 15 (2020).
[40] Y. Hasegawa, Thermodynamic Uncertainty Relation for General Open Quantum Systems, Phys. Rev. Lett. **126**, 010602 (2021).
[41] H. J. D. Miller, M. H. Mohammady, M. Perarnau-Llobet, and G. Guarnieri, Thermodynamic Uncertainty Relation in Slowly Driven Quantum Heat Engines, Phys. Rev. Lett. **126**, 210603 (2021).
[42] G. Falasco and M. Esposito, Dissipation-Time Uncertainty Relation, Phys. Rev. Lett. **125**, 120604 (2020).
[43] T. R. Gingrich and J. M. Horowitz, Fundamental Bounds on First Passage Time Fluctuations for Currents, Phys. Rev. Lett. **119**, 170601 (2017).
[44] I. Neri, É. Roldán, and F. Jülicher, Statistics of Infima and Stopping Times of Entropy Production and Applications to Active Molecular Processes, Phys. Rev. X **7**, 011019 (2017).
[45] I. Neri, Second Law of Thermodynamics at Stopping Times, Phys. Rev. Lett. **124**, 040601 (2020).
[46] S. Redner, *A Guide to First-Passage Processes* (Cambridge University Press, Cambridge, England, 2001).
[47] C. Forbes, M. Evans, N. Hastings, and B. Peacock, *Statistical Distributions* (John Wiley & Sons, New York, 2011).
[48] U. Seifert, Stochastic thermodynamics, fluctuation theorems and molecular machines, Rep. Prog. Phys. **75**, 126001 (2012).
[49] C. V. den Broeck and M. Esposito, Ensemble and trajectory thermodynamics: A brief introduction, Physica A (Amsterdam) **418**, 6 (2015).
[50] This dissipation-time uncertainty relation can also be applied to isolated systems. For an isolated system initially in a nonequilibrium state, the entropy flow would occur between different parts of the system, in which the time reversed process is exponentially rare. Thus the corresponding entropy rate is bounded by the dissipation-time uncertainty relation of Eqs. (1) or (2).
[51] See Supplemental Material at http://link.aps.org/supplemental/10.1103/PhysRevLett.128.050603 for more details, which includes Refs. [2,42].
[52] P. Hänggi, P. Talkner, and M. Borkovec, Reaction-rate theory: Fifty years after Kramers, Rev. Mod. Phys. **62**, 251 (1990).
[53] M. B. Plenio and P. L. Knight, The quantum-jump approach to dissipative dynamics in quantum optics, Rev. Mod. Phys. **70**, 101 (1998).